Nanowires

DOI: 10.1002/ange.200601588

Luminescent One-Dimensional Nanoscale Materials with $Pt^{II}\cdots Pt^{II}$ Interactions**

Yinghui Sun, Kaiqi Ye, Hongyu Zhang, Junhu Zhang, Lan Zhao, Bao Li, Guangdi Yang, Bai Yang, Yue Wang, Siu-Wai Lai, and Chi-Ming Che**

Self-assembly of organic and inorganic molecules into one-dimensional (1D) micrometer- and nanometer-scale architectures has become a useful approach for the fabrication of materials with extraordinary properties and applications.[1–12] Noncovalent intermolecular interactions are widely regarded as an efficient approach to construct molecular assemblies with well-defined structures in the micro- and nanoscopic size regime and involve hydrogen-bonding, π–π stacking, electrostatic, and van der Waals interactions. The size and structure of nanoscale aggregates can be significantly varied through manipulation of intermolecular interactions by the judicious choice of the solvent and/or functionalization of the precursor molecules.[3–7] On the contrary, the use of weak metal⋯metal interactions in the construction of 1D nanostructures remains sparse.[13] Herein, we report luminescent 1D inorganic micro- and nanowires from $[Pt(CN\textit{t}Bu)_2(CN)_2]$ that are aggregated and directed by $Pt^{II}\cdots Pt^{II}$ interactions. The precursor $[Pt(CN\textit{t}Bu)_2(CN)_2]$ was synthesized in high yield by stirring K_2PtCl_4 and excess *tert*-butyl isocyanide in water at room temperature.[14] This partially dealkylated complex is stable towards air and moisture at room temperature. Slow diffusion of diethyl ether vapor into a solution of $[Pt(CN\textit{t}Bu)_2(CN)_2]$ in acetonitrile resulted in the formation of light green, long rodlike crystals, which exhibit strong green emission under UV light (Figure 1).

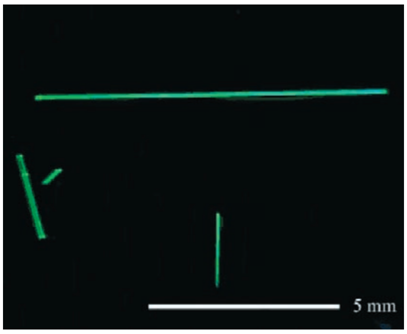

Figure 1. Photographic image of $[Pt(CN\textit{t}Bu)_2(CN)_2]$ crystals excited with UV light ($\lambda_{ex} = 365$ nm).

The molecular structure of $[Pt(CN\textit{t}Bu)_2(CN)_2]$ was determined by X-ray crystallography (Figure 2). The two CN and CN*t*Bu ligands respectively adopt *cis* geometry (Figure 2a). In the crystal packing diagram, $[Pt(CN\textit{t}Bu)_2(CN)_2]$ units stack in pairs along the *a* axis with a C(8)-Pt(1)-Pt(2)-C(4) torsion angle of 125.20° (Figure 2b), and this pattern extends continuously with adjacent pairs to form infinite linear stacks of square-planar Pt^{II} molecules along the *a* axis with $Pt^{II}\cdots Pt^{II}$ distances of 3.354(1) Å. This pattern is similar to those observed in other extended linear-chain platinum(II) complexes.[15] Figure 2c displays a view of a $[Pt]_n$ chain aligned as a 1D coordination wire. The $[Pt]_n$ chains are packed along the *a* axis to result in the formation of rod-type crystals (Figure 2d). Nonclassical hydrogen bonding for the intermolecular C–H⋯N≡C interactions are observed (H⋯N 2.66–2.74 Å; angle C–H⋯N 144.9–154.2°; see Supporting Information), through which bundles of $[Pt]_n$ chains are held together in the crystal structure of $[Pt(CN\textit{t}Bu)_2(CN)_2]$ (see Supporting Information). These structural features encouraged us to explore the possibility of employing $[Pt(CN\textit{t}Bu)_2(CN)_2]$ as a building block for the construction of 1D micrometer- and nanometer-sized wires and fibers based on $Pt^{II}\cdots Pt^{II}$ interactions.

First, an evaporation approach was employed for the aggregation of $[Pt(CN\textit{t}Bu)_2(CN)_2]$ molecules into luminescent wires. Following evaporation of a solution of $[Pt(CN\textit{t}Bu)_2(CN)_2]$ in acetonitrile (10^{-4} M) in air on a silicon substrate, an emission microscope image was recorded that revealed the formation of wires assembled with high length/diameter aspect ratios (Figure 3a). The diameter of the Pt^{II} wires generated is approximately 25 μm, and their lengths can be more than 1000 μm. To obtain luminescent wires with smaller diameters, an approach of injection reprecipitation was employed. Luminescent wires of micrometer and nanometer diameters were prepared by controlling the volume of the solution of the complex in acetonitrile injected into water. Figure 3b and c show the topographic features of luminescent wires observed by optical microscopy and scanning electron

---

[*] Y. Sun, K. Ye, H. Zhang, J. Zhang, L. Zhao, B. Li, G. Yang, B. Yang, Prof. Dr. Y. Wang
Key Laboratory for Supramolecular Structure and Materials of the Ministry of Education
College of Chemistry
Jilin University
Changchun 130012 (P.R. China)
Fax: (+86) 431-519-3421
E-mail: yuewang@jlu.edu.cn
Dr. S.-W. Lai, Prof. Dr. C.-M. Che
Department of Chemistry and
HKU-CAS Joint Laboratory on New Materials
University of Hong Kong
Pokfulam Road, Hong Kong SAR (P.R. China)
Fax: (+852) 2857-1586
E-mail: cmche@hku.hk

[**] This work was supported by the National Natural Science Foundation of China, the Major State Basic Research Development Program (2002CB613401), and the Program for Changjiang Scholars and Innovative Research Teams in Universities (IRT0422). We are grateful for financial support from the Research Grants Council of the Hong Kong SAR, China (HKU 7039/03P), the National Natural Science Foundation of China/Research Grants Council Joint Research Scheme (N HKU 742/04), and the University Development Fund (Nanotechnology Research Institute Program) and Strategic Research Theme (Nano-biotechnology) of the University of Hong Kong.

Supporting information for this article is available on the WWW under http://www.angewandte.org or from the author.

microscopy (SEM), respectively. The diameter of the wires formed was sensitive to the volume of the solution: 200 μL of $[\mathrm{Pt(CN}t\mathrm{Bu)_2(CN)_2}]$ in acetonitrile afforded luminescent wires with diameters of around 500 nm, whereas 50 μL of the solution gave wires with diameter of approximately 70 nm.

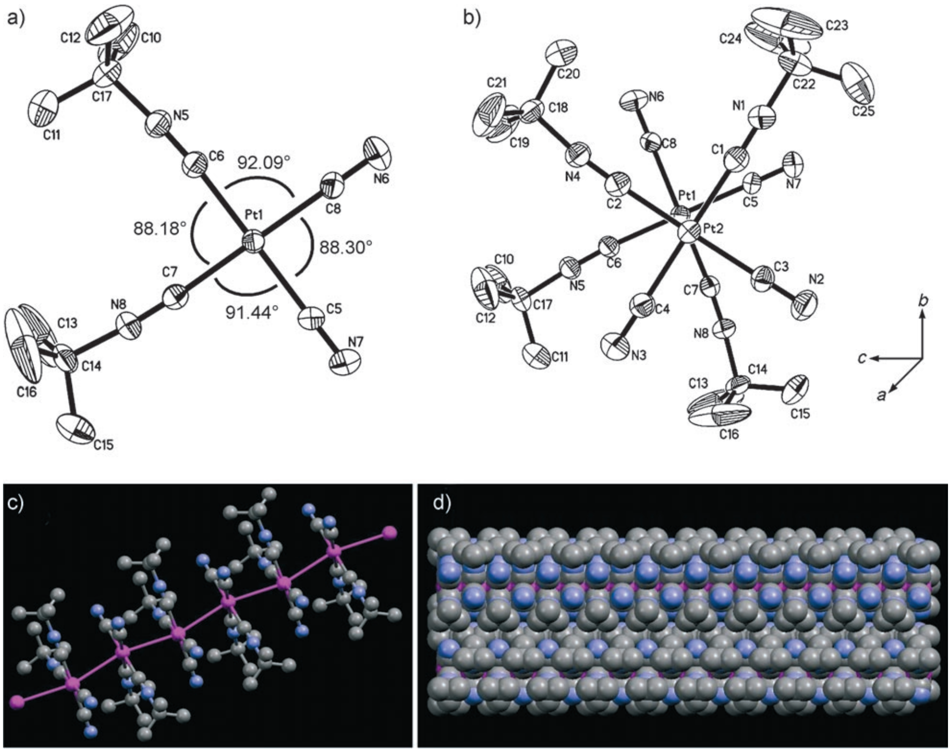

Figure 2. Crystal structure of $[\mathrm{Pt(CN}t\mathrm{Bu)_2(CN)_2}]$. a) ORTEP drawing with thermal ellipsoids shown at the 30% probability level. b) View along the *a* axis showing the relative orientation of two adjacent $[\mathrm{Pt(CN}t\mathrm{Bu)_2(CN)_2}]$ molecules (H atoms labels omitted for clarity). c) Side view of molecular wire showing metal–metal interactions (Pt pink, N blue, C gray). d) Crystal packing diagram of $[\mathrm{Pt}]_n$ chains.

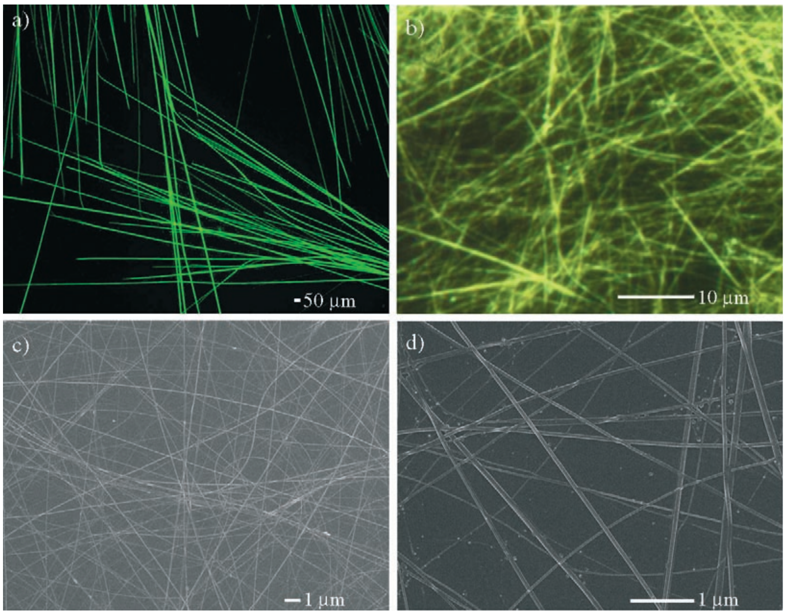

Figure 3. Emission microscopy images (a, b; upon excitation at 365 nm) and scanning electron micrographs (c, d; under different magnification) of luminescent $[\mathrm{Pt(CN}t\mathrm{Bu)_2(CN)_2}]$ wires formed a) on a silicon substrate by slowly evaporating a solution of $[\mathrm{Pt(CN}t\mathrm{Bu)_2(CN)_2}]$ in acetonitrile (10^{-4} M); by injecting 200 μL (b) and 50 μL (c, d) of a solution of $[\mathrm{Pt(CN}t\mathrm{Bu)_2(CN)_2}]$ in acetonitrile (9.6×10^{-3} M) into 10 mL of water followed by transferring the mixture onto a silicon substrate. In parts (c, d), a platinum layer was sputtered onto the surface to increase the conductivity.

Upon excitation at 365 nm with a UV lamp, $[\mathrm{Pt(CN}t\mathrm{Bu)_2(CN)_2}]$ nanowires exhibited an intense emission at $\lambda_{\max} = 560$ nm at 298 K (see Supporting Information). However, when the wires were dissolved in acetonitrile a colorless solution was obtained. Figure 4a shows the emission spectra of a solution of $[\mathrm{Pt(CN}t\mathrm{Bu)_2(CN)_2}]$ in acetonitrile recorded at different temperatures (from 298 to 77 K). At 298 K the solution was nonemissive, but an emission with $\lambda_{\max} = 542$ nm developed at a temperature of 220 K. Upon lowering the temperature, aggregation of $[\mathrm{Pt(CN}t\mathrm{Bu)_2(CN)_2}]$ in acetonitrile at 220 K was observed, and the emission at $\lambda = 542$ nm is attributed to the $^3[5d_\sigma{}^*, 6p_\sigma]$ electronic excited state of $[\mathrm{Pt(CN}t\mathrm{Bu)_2(CN)_2}]$ aggregates.[16–18] As the temperature of the solution of $[\mathrm{Pt(CN}t\mathrm{Bu)_2(CN)_2}]$ was further decreased to 77 K, the emission at $\lambda = 542$ nm was resolved into two bands at 584 and 530 nm with lifetimes (τ) of 2.5 and 3.5 μs, respectively. Variation of the excitation wavelength resulted in a change in the relative intensity of the two emission bands at 530 and 584 nm (see Supporting Information). These results suggest that the emissions at $\lambda = 530$ and 584 nm originate from different $[\mathrm{Pt(CN}t\mathrm{Bu)_2(CN)_2}]_\mathrm{n}$ species. Previous work revealed that the emission properties of $[\mathrm{Pt(CN)_4}]^{2-}$ in solution are affected by the concentration of the complex and can be attributed to the $^1[5d_\sigma{}^*, 6p_\sigma]$ and $^3[5d_\sigma{}^*, 6p_\sigma]$ excited states of $\{[\mathrm{Pt(CN)_4}]^{2-}\}_n$ for different values of n.[19] The emission spectra of $[\mathrm{Pt(CN}t\mathrm{Bu)_2(CN)_2}]$ nanowires showed a temperature dependence (Figure 4b) similar to that recorded in acetonitrile solution. The solid-state emission at 562 nm at 298 K resolved into two peak maxima at 545 and 597 nm upon decreasing the temperature to 77 K. We also found that the emission spectrum of [Pt-

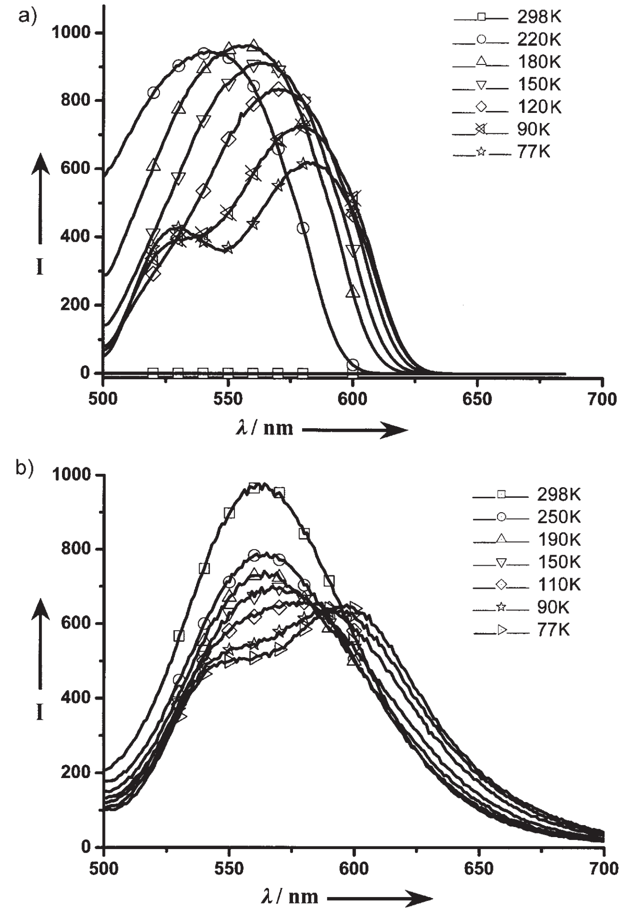

Figure 4. Emission spectra of a) a solution of $[Pt(CNtBu)_2(CN)_2]$ in acetonitrile (5.0×10^{-4} M) and b) $[Pt(CNtBu)_2(CN)_2]$ nanowires at different temperatures. The nanowires were formed by injecting 200 µL of a solution of $[Pt(CNtBu)_2(CN)_2]$ in acetonitrile (9.6×10^{-3} M) into 10 mL of water followed by transferring the mixture onto a silicon substrate.

$(CNtBu)_2(CN)_2]$ nanowires at 77 K depends on the excitation wavelength (see Supporting Information).

The relationships between the excitation and emission spectra were examined. For a glassy solution of $[Pt(CNtBu)_2(CN)_2]$ in benzonitrile (5.66×10^{-5} M) at 77 K, the emission spectra recorded at different excitation wavelengths showed a gradual shift in emission maximum (see Supporting Information). Upon excitation of the glassy solution at 475 nm, an emission peak at 547 nm and a shoulder at 610 nm were observed. Upon shifting the excitation wavelength to higher energy, the corresponding emission maximum was also blue-shifted. A series of excitation spectra were recorded while monitoring different emission wavelengths: an intense band was found with a spectral profile resembling the $[nd_\sigma^*\rightarrow(n+1)p_\sigma]$ transition of dinuclear d^8 or d^{10} metal systems,[16,20] and the excitation peak maximum shifted from 480 nm to 464, 452, 433, and 428 nm upon changing the emission wavelength from 570 nm to 547, 534, 520, and 502 nm, respectively. We tentatively assign the different photophysical properties to the $[5d_\sigma^*\rightarrow6p_\sigma]$ electronic excited states of $[Pt(CNtBu)_2(CN)_2]_n$ aggregates.

Exposure of $[Pt(CNtBu)_2(CN)_2]$ nanowires to the vapor of volatile organic compounds (VOCs) resulted in changes in the emission properties (Figure 5). A shift of the emission maximum from 562 to 533 nm was observed with a concomitant increase in emission intensity. Such solvatochromism was reversible, and the emission spectrum was restored to its original profile after the sample was placed in air for 15 days or under vacuum for 10 h. Subtle environmental changes can perturb the weak $Pt^{II}\cdots Pt^{II}$ interactions and subsequently affect the $^3[5d_\sigma^*,6p_\sigma]$ emissive properties.[16–18] Previous studies have demonstrated that the $^3[5d_\sigma^*,6p_\sigma]$ excited states of dinuclear and linear-chain Pt^{II} compounds are sensitive to temperature and atmospheric factors.[15a,17,21,22] Here, we examined the vapochromic behavior of the crystals obtained by diffusing diethyl ether vapor into a solution of $[Pt(CNtBu)_2(CN)_2]$ in acetonitrile. These bright yellow crystals of $[Pt(CNtBu)_2(CN)_2]$ in the dry state showed an intense emission with $\lambda_{max} = 534$ nm ($\tau = 0.85$ µs; quantum yield $\Phi = 0.33$) at 298 K, however, at 77 K two emission peaks with maxima at $\lambda = 510$ ($\tau = 0.47$ µs) and 569 nm ($\tau = 1.65$ µs) were observed. Exposure of the crystals to acetonitrile vapor only resulted in a change in the emission intensity with no shift of the emission maximum (see Supporting Information). We propose that the micro- and nanostructures of $[Pt(CNtBu)_2(CN)_2]$ species exhibit large surface areas, which would enhance the contact between $[Pt(CNtBu)_2(CN)_2]$ molecules and the organic solvent molecules.

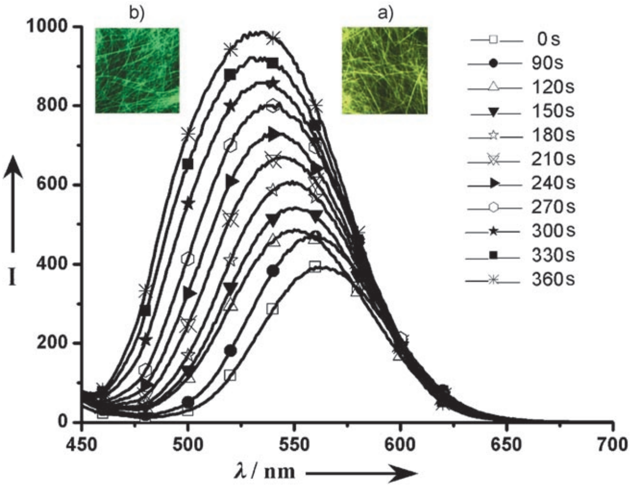

Figure 5. Room-temperature emission spectra of $[Pt(CNtBu)_2(CN)_2]$ nanowires recorded after exposure of the sample to acetonitrile vapor at different time intervals. The wires were formed by injecting 200 µL of a solution of $[Pt(CNtBu)_2(CN)_2]$ in acetonitrile (9.6×10^{-3} M) into 10 mL of water followed by transferring the mixture onto a silicon substrate. Insets: Emission microscopy images of luminescent wires before (a) and after (b) exposure to acetonitrile vapor.

To examine the effect of acetonitrile vapor upon the crystal structure and packing of $[Pt(CNtBu)_2(CN)_2]$, X-ray diffraction data were collected under different conditions. Crystals were grown by diffusion of diethyl ether into a solution of $[Pt(CNtBu)_2(CN)_2]$ in acetonitrile at room temperature. Crystal **1** was isolated from the solution mixture (acetonitrile and diethyl ether) and kept in air at room temperature for 15 days, and the X-ray crystal data were collected at 298 K. Crystal **2** was isolated from the solution and encapsulated in epoxy resin, and the X-ray data were immediately recorded at 298 K. For crystal **2**, although we could not precisely locate the coordinates of some carbon and nitrogen atoms at 298 K, the coordinates of the Pt atom and coordinated carbon atoms could be accurately determined. On the basis of the two sets of X-ray crystal data, the intermolecular $\mathrm{Pt^{II}}\cdots\mathrm{Pt^{II}}$ distances in the two structures were found to be similar (3.354(1) Å for crystal **1**; 3.3525(2) Å for crystal **2**) but there are slight variations in the bond angles (∢*t*BuNC-Pt-CN*t*Bu = 88.18° for crystal **1** and 92.11° for crystal **2**; ∢NC-Pt-CN = 88.30° (**1**) and 98.52° (**2**); ∢*t*BuNC-Pt-CN = 91.44, 92.09° (**1**) and 83.46, 85.91° (**2**)) around the $\mathrm{Pt^{II}}$ center (see Supporting Information). This observation is consistent with the finding that exposure of dry crystals of $[\mathrm{Pt(CN}t\mathrm{Bu)_2(CN)_2}]$ to acetonitrile vapor affects the emission intensity, but the variation in the emission maximum is small (see Supporting Information).

In conclusion, we have demonstrated that $[\mathrm{Pt(CN}t\mathrm{Bu)_2(CN)_2}]$ molecules can form micrometer- and nanometer-scale luminescent wires. Weak $\mathrm{Pt^{II}}\cdots\mathrm{Pt^{II}}$ interactions are useful cohesive force for the construction of 1D functional nanomaterials. Recent work has revealed that 1D nanorods can be obtained from cyclometalated platinum(II) complexes.[13b] More importantly, $\mathrm{Pt^{II}}\cdots\mathrm{Pt^{II}}$ interactions not only induce the formation of 1D nanostructures but are also responsible for the intense green $^3[5d_{\sigma}^*,6p_{\sigma}]$ emission of the self-assembled $[\mathrm{Pt(CN}t\mathrm{Bu)_2(CN)_2}]$ wires.

Received: April 22, 2006
Revised: June 21, 2006

Keywords: cyanides · luminescence · metal–metal interactions · nanostructures · platinum

---

[1] J. P. Hill, W. Jin, A. Kosaka, T. Fukushima, H. Ichihara, T. Shimomura, K. Ito, T. Hashizume, N. Ishii, T. Aida, *Science* **2004**, *304*, 1481–1483.

[2] J. Huang, R. B. Kaner, *J. Am. Chem. Soc.* **2004**, *126*, 851–855.

[3] B.-K. An, D.-S. Lee, J.-S. Lee, Y.-S. Park, H.-S. Song, S. Y. Park, *J. Am. Chem. Soc.* **2004**, *126*, 10232–10233.

[4] P. Yan, A. Chowdhury, M. W. Holman, D. M. Adams, *J. Phys. Chem. B* **2005**, *109*, 724–730.

[5] R. Harada, Y. Matsuda, H. Okawa, T. Kojima, *Angew. Chem.* **2004**, *116*, 1861–1864; *Angew. Chem. Int. Ed.* **2004**, *43*, 1825–1828.

[6] M. L. Bushey, T.-Q. Nguyen, C. Nuckolls, *J. Am. Chem. Soc.* **2003**, *125*, 8264–8269.

[7] T.-Q. Nguyen, R. Martel, P. Avouris, M. L. Bushey, L. Brus, C. Nuckolls, *J. Am. Chem. Soc.* **2004**, *126*, 5234–5242.

[8] K. L. Niece, J. D. Hartgerink, J. J. J. M. Donners, S. I. Stupp, *J. Am. Chem. Soc.* **2003**, *125*, 7146–7147.

[9] H. Fu, D. Xiao, J. Yao, G. Yang, *Angew. Chem.* **2003**, *115*, 2989–2992; *Angew. Chem. Int. Ed.* **2003**, *42*, 2883–2886.

[10] H. Liu, Q. Zhao, Y. Li, Y. Liu, F. Lu, J. Zhuang, S. Wang, L. Jiang, D. Zhu, D. Yu, L. Chi, *J. Am. Chem. Soc.* **2005**, *127*, 1120–1121.

[11] H. Liu, Y. Li, S. Xiao, H. Gan, T. Jiu, H. Li, L. Jiang, D. Zhu, D. Yu, B. Xiang, Y. Chen, *J. Am. Chem. Soc.* **2003**, *125*, 10794–10795.

[12] H. Yao, C. A. Michaels, S. J. Stranick, T. Isohashi, K. Kimura, *Lett. Org. Chem.* **2004**, *1*, 280–287.

[13] a) M. Enomoto, A. Kishimura, T. Aida, *J. Am. Chem. Soc.* **2001**, *123*, 5608–5609; b) W. Lu, V. A. L. Roy, C.-M. Che, *Chem. Commun.* **2006**, DOI:10.1039/B607422G.

[14] L. Malatesta, F. Bonati, *Isocyanide Complexes of Metals*, Wiley, London, **1969**, p. 169.

[15] a) C. E. Buss, K. R. Mann, *J. Am. Chem. Soc.* **2002**, *124*, 1031–1039; b) V. W.-W. Yam, K. M.-C. Wong, N. Zhu, *J. Am. Chem. Soc.* **2002**, *124*, 6506–6507.

[16] D. M. Roundhill, H. B. Gray, C. M. Che, *Acc. Chem. Res.* **1989**, *22*, 55–61.

[17] B.-H. Xia, C.-M. Che, D. L. Phillips, K.-H. Leung, K.-K. Cheung, *Inorg. Chem.* **2002**, *41*, 3866–3875.

[18] C.-M. Che, L. G. Butler, H. B. Gray, R. M. Crooks, W. H. Woodruff, *J. Am. Chem. Soc.* **1983**, *105*, 5492–5494.

[19] J. W. Schindler, R. C. Fukuda, A. W. Adamson, *J. Am. Chem. Soc.* **1982**, *104*, 3596–3600.

[20] a) S.-W. Lai, H.-W. Lam, W. Lu, K.-K. Cheung, C.-M. Che, *Organometallics* **2002**, *21*, 226–234; b) W.-F. Fu, K.-C. Chan, K.-K. Cheung, C.-M. Che, *Chem. Eur. J.* **2001**, *7*, 4656–4664.

[21] C. L. Exstrom, J. R. Sowa, Jr., C. A. Daws, D. Janzen, K. R. Mann, G. A. Moore, F. F. Stewart, *Chem. Mater.* **1995**, *7*, 15–17.

[22] C. E. Buss, C. E. Anderson, M. K. Pomije, C. M. Lutz, D. Britton, K. R. Mann, *J. Am. Chem. Soc.* **1998**, *120*, 7783–7790.